CONTENT

1. ELECTROMAGNETIC AND MECHANICAL FUNDAMENTALS 3
1.1. Introduction 3
1.2. Moment of inertia 3
1.3. Friction 7
1.4. Path control 8
1.4.1. Straight cut 8
1.4.2. Point-to-point (Trapezoidal) 8
1.4.3. Point-to-point (Triangular) 9
1.4.4. Contouring (e.g. in rotational motion) 10
1.5. Power transmission (linkage) 11
1.6. Rotational motion dynamics and kinetic energy 17
1.7. Magnetic field and magnetomotive force 18
1.8. Transformer 19
1.9. Tutorial 21
2. POWER ELECTRONIC CONTROL OF DC MOTOR DRIVES 22
2.1. Introduction 22
2.2. Fundamentals of DC machines 23
2.3. Speed control of separately excited DC motors 25
2.4. Rectifier Control of separately excited DC motors 28
2.5. Chopper control of DC machines 32
2.6. Regenerative braking 35
2.7. Tutorial 39
3. POWER ELECTRONIC CONTROL OF AC INDUCTION MOTOR DRIVES 41
3.1. Introduction 41
3.2. Fundamentals of AC induction machines 41
3.3. Speed control by simultaneous stator voltage and frequency variation 49
3.4. Inverter control of induction machines using sinusoidal PWM 52
3.5. Dynamic control of induction machines using voltage source inverters (an introduction) 55
3.6. Tutorial 56
4. SIZING OF ELECTRIC DRIVES 58
4.1. Introduction 58
4.2. Turning process 58
4.3. Milling process 60
4.4. Tutorial 60
4.5. Appendix 61

Reference

[1] M. H. Rashid. *Power Electronics – Circuits, Devices, and Applications*, 3rd ed. Pearson. 2003.

[2] Emil Levi. *Power Electronics, Drives and Systems*. Course material. 2014.

[3] Richard Crowder. *Electric Drives and Electromechanical Systems.* Elsevier. 2006.

3. POWER ELECTRONIC CONTROL OF AC INDUCTION MOTOR DRIVES

3.1. Introduction

AC motors are usually 20%-40% lighter than the equivalent DC machines, less expensive, robust, and require low maintenance. The range of AC motors include the induction motor (squirrel-cage or wound-rotor), synchronous motor (wound rotor, permanent magnet), synchronous and switched reluctance motor, and etc. Nevertheless, AC motors exhibit highly coupled (magnetic coupling among rotor and stator of all phases) and nonlinear (i.e. magnetic saturation effect) behavior as opposed to much simpler decoupled structures of separately excited dc motors. Therefore, the control of AC drives generally requires a more complex algorithms with fast switching power converters than that in DC drives. AC drives in general control the magnitude, frequency, and phase angle (for high performance AC drives) of the voltage and/or current to achieve variable speed application.

The focus of this chapter is first on the fundamentals of AC induction machines, which lays the theoretical consideration for scalar control method, a.k.a variable-voltage-variable-frequency-control method. Then, the state-of-the-art implementation of an AC drive through the use of voltage source inverter with pulse width modulation (PWM) technique is introduced. Lastly, vector control – being the high performance control methods for induction motors – will be briefly introduced but without detailed mathematical treatment (to commensurate with the second year subjects).

3.2. Fundamentals of AC induction machines

Three-phase induction motors have three-phase stator windings and, theoretically, also three-phase rotor windings. Ideally, the stator windings are supplied with a balanced three-phase supply which drives the flow of AC stator currents. These currents create a rotating magnetic flux in the small air gap between the stator and rotor, which then induces voltages in the rotor windings (Faraday's law). These induced back EMFs cause the flow of rotor currents which in turn create the rotating magnetic flux. The magnetic flux are coupled back to the stator windings and induces back EMFs at the stator windings. The interaction of the rotor current and the air-gap flux produces a torque on the rotor which is free to move. The rotor movement in turn affects the transformer-action between the stator and rotor described above. The rotor speed will increase to until close to the synchronous speed of the rotating stator magnetic flux. Perhaps this simple description hints about the complex electrical dynamics inside an AC induction motor.

There are two categories of induction motor: wound-rotor type and squirrel cage type. Would-rotor induction motor has physical rotor windings (which physically rotate as the rotor moves) that are accessible through slip rings. This motor was popular before the wide spread of AC drives as the accessible rotor windings allow external resistance to be connected for starting and speed control purposes (to be descried later). Squirrel-cage induction motor on the other hand, occupies the largest share of AC motors of all types in the industry thanks to the low cost, low maintenance, and robust properties. For both types of induction motors, the stator structure is exactly the same but the squirrel-cage type has a casted squirrel-cage-like aluminum/copper conductors that has two rings at both ends and multiple straight bars connected between the two rings' peripheral. The space between the rings are filled with stacked laminated steel. This structure is illustrated in Fig. 3.1. Fig. 3.2 shows the cross-sectional view of a squirrel-cage induction motor.

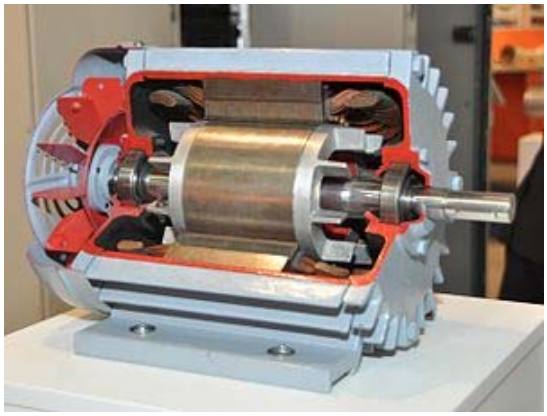

Fig. 3.1: Squirrel-cage induction motor.

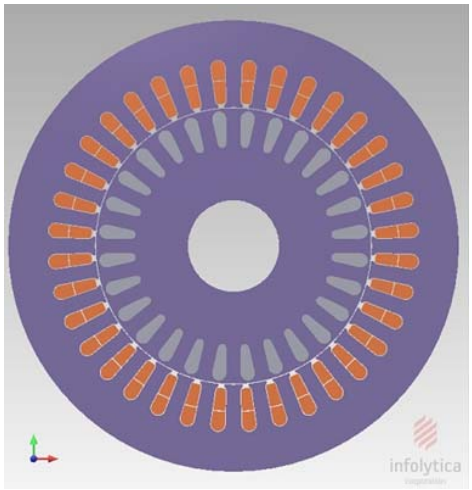

Fig. 3.2: Cross-sectional view of an induction motor [www.infolytica.com].

The following section analyses the steady-state model of the induction motor. To start with, the speed of rotation of the magnetic field due to the stator currents is known as the synchronous speed, and it is defined as:

$$\omega_s = \frac{\omega}{P}$$

where ω is the supply frequency $2\pi f$, in rads^{-1}, and P is the pole pairs ($P = p/2$, where p is the number of poles, and f is the supply frequency, in Hz). Alternatively, the synchronous speed can be expressed as $60f/P$ or $120f/p$, in revolution per minute (rpm). Another important parameter, s, which is the slip of the motor, is defined as:

$$s = \frac{\omega_s - \omega_m}{\omega_s}$$

Motor speed can be found from $\omega_m = \omega_s(1 - s)$.

If a stator phase voltage $v_s = V_{pk}\sin \omega_s t$ produces steady-state magnetic flux linkage $\phi(t)$ in the rotor at a given speed ω_m:

$$\phi(t) = \phi_{pk} \cos(\omega_m t + \delta - \omega_s t)$$

Then the induced back EMF at one phase of the rotor windings with an equivalent N_r turns is (assuming that ω_s and ω_m are constant):

$$\begin{aligned} e_r(t) &= \frac{d(N_r\phi(t))}{dt} \\ &= N_r \frac{d}{dt}\left(\phi_{pk}\cos(\omega_m t + \delta - \omega_s t)\right) \\ &= -N_r\phi_{pk}(\omega_m - \omega_s)\sin[(\omega_m - \omega_s)t + \delta] \\ &= -N_r\phi_{pk}(\omega_s - \omega_m)\sin\left[(\omega_s - \omega_m)t - \delta\right] \\ &= -s\omega_s N_r\phi_{pk}\sin(s\omega_s t - \delta) \\ &= -sE_{pk}\sin(s\omega_s t - \delta) \\ &= -s\sqrt{2}E_r\sin(s\omega_s t - \delta) \end{aligned}$$

where
N_r = number of turns on each rotor phase
ω_m = angular speed of the rotor
ω_s = synchronous speed of the motor
δ = relative position of the rotor
$E_{pk} = N_r\phi_{pk}\omega_s$ = peak value of the rotor induced back EMF
E_r = rms value of the rotor induced back EMF

From the rotor back EMF expression, it can be noticed that when the motor is at standstill, i.e. $\omega_m = 0$ and therefore slip $s = 1$, the induced back EMF in the rotor has the maximum amplitude of E_{pk}; when the motor is rotating at the synchronous speed $\omega_m = \omega_s$ and therefore slip $s = 0$, the induced back EMF in the rotor has zero amplitude. Frequency of the induced back EMF in the rotor is the difference between the synchronous speed and rotor speed.

Steady-state operation of a balanced three-phase induction motor can be analyzed by simply referring to the single-phase circuitry known commonly as the per-phase equivalent circuit, as shown in Fig. 3.3. This circuit is the transformer model of an induction motor.

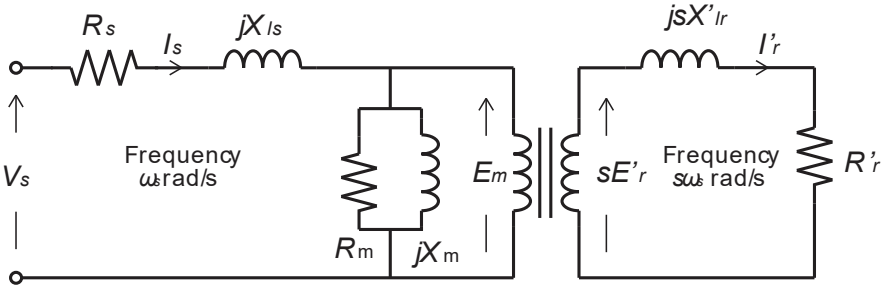

Fig. 3.3: Per-phase equivalent circuit of a three-phase squirrel-cage induction motor. The rotor circuit refers to the rotor winding itself. These are the actual, physical parameters measurable at the rotor.

Manipulate the rotor current expressed in rms phasors:

$$\boldsymbol{I}_{\boldsymbol{r}}^{'} = \frac{s\boldsymbol{E}_{\boldsymbol{r}}^{'}}{R_r^{'} + jsX_{lr}^{'}}$$
$$= \frac{\boldsymbol{E}_{\boldsymbol{r}}^{'}}{R_r^{'}/s + jX_{lr}^{'}}$$

With reference to the result, the rotor circuit's frequency base can be modified accordingly to the one shown in Fig. 3.4, which has all the speed variation effects concentrated in the rotor impedance term.

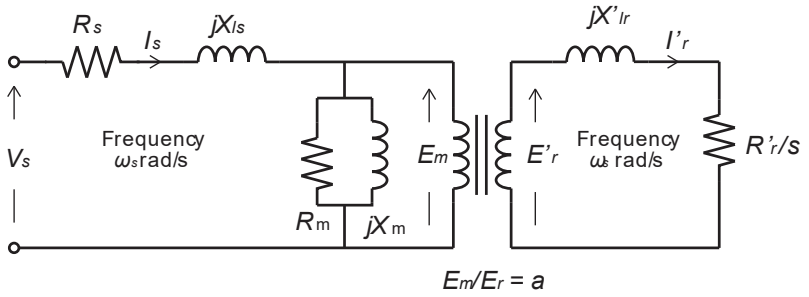

Fig. 3.4: Per-phase equivalent circuit of a three-phase squirrel-cage induction motor. The rotor circuit's frequency has been changed from the slip frequency to the synchronous frequency.

Lastly, by adjusting E'_r using the stator/rotor winding ratio a (see section 1.8 for details), an equivalent circuit with all parameters referencing to the stator winding is shown in Fig. 3.5.

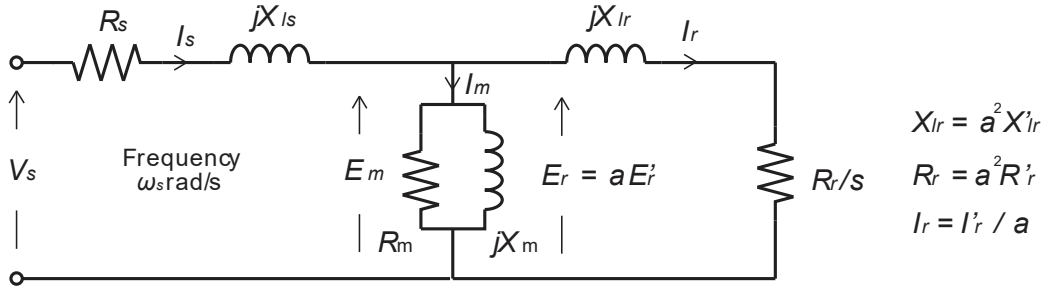

Fig. 3.5: The complete per-phase equivalent circuit of a three-phase induction motor with reference only to the stator winding.

V_s is the rated phase to neutral rms voltage of the stator. All the reactance are at the rated frequency. Using the basic circuit theory, the following basic performance indictor of a three-phase induction motor can be derived:

Air-gap power (power transferred from the stator to the rotor) $P_{ag} = 3I_r^2 \frac{R_r}{s}$

Stator copper loss $P_{scloss} = 3I_s^2 R_s$

Rotor copper loss $P_{rcloss} = 3I_r^2 R_r$

Core loss $P_{core-loss} = \frac{3E_m^2}{R_m} \approx \frac{3V_s^2}{R_m}$

Total input active power is:

$$\begin{aligned} P_{in} &= 3V_s^2 I_s \cos\theta_m \\ &= P_{core-loss} + P_{scloss} + P_{ag} \end{aligned}$$

where θ_m is the phase angle between phasor V_s and I_s. The developed mechanical power is:

$$\begin{aligned} P_{mech} &= P_{ag} - P_{rcloss} \\ &= 3I_r^2 \frac{R_r}{s} - 3I_r^2 R_r \\ &= 3I_r^2 R_r \frac{(1-s)}{s} \\ &= P_{ag}(1-s) \end{aligned}$$

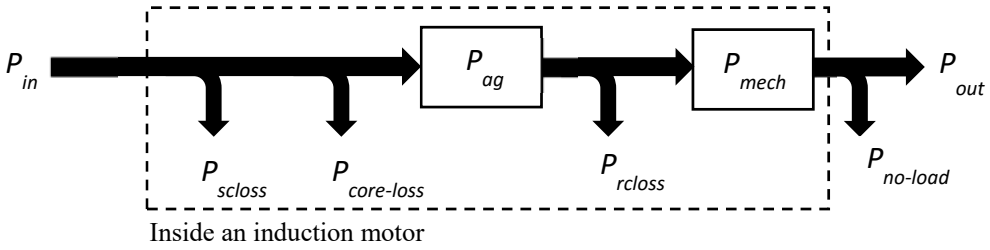

Fig. 3.6: Power components during the energy conversion process inside an induction motor.

Useful output power is the difference between the developed mechanical power and the power to overcome the mechanical friction and windage loss (i.e. the no-load power):

$$P_{out} = P_{mech} - P_{no-load}$$

The electrical-to-mechanical power conversion efficiency of the induction motor can be estimated from

$$\begin{aligned} \eta &= \frac{P_{mech}}{P_{in}} \\ &= \frac{P_{mech}}{P_{core-loss} + P_{scloss} + P_{ag}} \end{aligned}$$

By assuming $P_{ag} >> P_{core\text{-}loss}$ and $P_{ag} >> P_{scloss}$, we get:

$$\begin{aligned} \eta &\approx \frac{P_{mech}}{P_{ag}} \\ &= \frac{P_{ag}(1-s)}{P_{ag}} \\ &= (1-s) \end{aligned}$$

Lastly, if the useful-power-to-input-power efficiency of the induction motor is of interest, it can be calculated from:

$$\eta = \frac{P_{out}}{P_{in}}$$

By equating the P_{mech} expression with $T_e\omega_m$, the T_e expression can be found in terms of I_r (and other parameters). However, I_r is of less interest as it is usually not measureable due to the closed squirrel-cage rotor structure. Hence the I_r expression in terms of V_s is first to be found as follows. The value of R_m is usually very large and hence it is often not considered in typical non-core-loss related calculation.

Next, we would like to determine the relationship between I_r and the slip speed s. There are several ways to achieve this: by assuming that X_m is very large (e.g. tens of times) larger than $|R_s + jX_{ls}|$, then one can assume with a rated voltage supply that $V_s \approx V_m$; alternatively, more accurately, one can use Thevenin equivalent circuit to simplify the circuit consisting the stator impedance R_s+jX_{ls} and the magnetizing reactance X_m to an equivalent circuit in series with the rotor circuit. What follows makes use of the Thevenin equivalent circuit, as in Fig. 3.7.

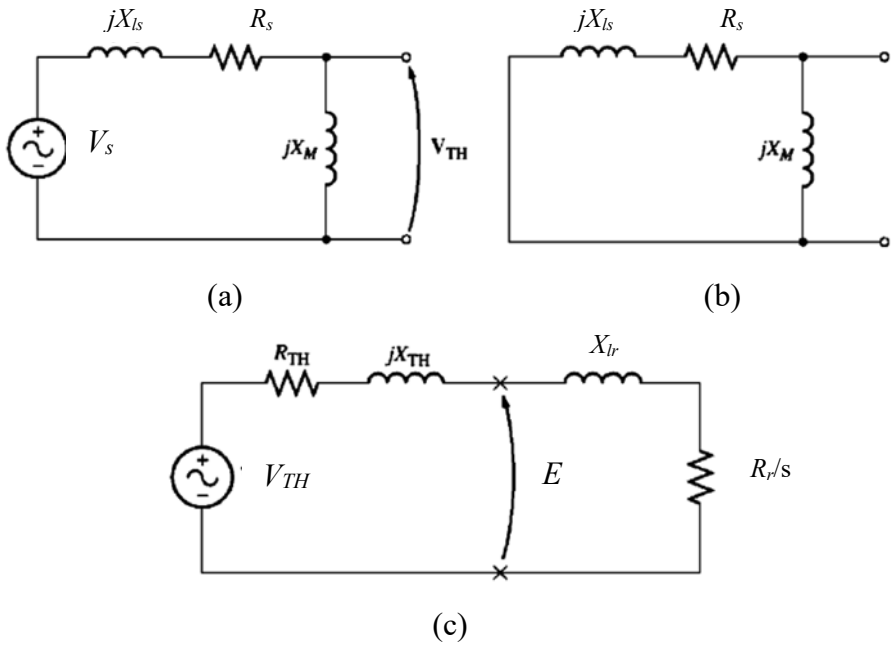

Fig. 3.7: Approximate per-phase equivalent circuit for a simpler torque/rotor-current expression. (a) To determine the Thevenin's voltage; (b) To determine the Thevenin's impedance; (c) Replacing the stator supply, the stator circuit, and the magnetizing circuits with the Thevenin's circuit.

The Thevenin equivalent circuit for the portion of circuitry shown in Fig. 3.7(a) is:

$$\boldsymbol{V_{TH}} = \frac{jX_M}{R_s + jX_{ls} + jX_M}\boldsymbol{V_s}$$

$$V_{TH} = \frac{X_M}{\sqrt{R_s^2 + (X_M + X_{ls})^2}}V_s$$

Based on Fig. 3.7(b), and assume that $X_M >> X_{ls}$ and $(X_M + X_{ls}) >> R_s$:

$$
\begin{aligned}
\boldsymbol{Z_{TH}} &= \frac{jX_M(R_s + jX_{ls})}{R_s + j(X_M + X_{ls})} \\
&= \frac{(-X_M X_{ls} + jX_M R_s)\left[R_s - j(X_M + X_{ls})\right]}{R_s^2 + (X_M + X_{ls})^2} \\
&= \frac{X_M R_s (X_M + X_{ls}) - R_s X_M X_{ls} + j\left[X_M R_s R_s + X_M X_{ls}(X_M + X_{ls})\right]}{R_s^2 + (X_M + X_{ls})^2} \\
&\approx \frac{R_s X_M^2}{(X_M + X_{ls})^2} + \frac{j\left[R_s^2 X_M + X_{ls} X_M (X_M + X_{ls})\right]}{(X_M + X_{ls})^2} \\
&\approx \frac{R_s X_M^2}{(X_M + X_{ls})^2} + j\left[R_s^2 \frac{X_M}{(X_M + X_{ls})^2} + \frac{X_{ls} X_M (X_M + X_{ls})}{(X_M + X_{ls})^2} \right] \\
&\approx \frac{R_s X_M^2}{(X_M + X_{ls})^2} + j\left[R_s \frac{R_s}{(X_M + X_{ls})} + X_{ls} \right] \\
&\approx R_s \left(\frac{X_M}{X_M + X_{ls}} \right)^2 + jX_{ls} \\
&= R_{TH} + jX_{TH}
\end{aligned}
$$

On the other hand, the magnetizing branch's voltage E can be expressed in terms of the Thevenin parameters as:

$$\boldsymbol{E} = \frac{R_r/s + jX_{lr}}{R_{TH} + R_r/s + j(X_{TH} + X_{lr})} \boldsymbol{V_s}$$

In most cases, one can assume that R_{TH} being R_s and V_{TH} being V_s, especially when X_m is not available. This form is usually more useful in steady-state analysis than the accurate form without the above approximation (not shown). The rotor current magnitude can be calculated from:

$$\boldsymbol{I_r} = \frac{\boldsymbol{V_{TH}}}{R_{TH} + R_r/s + j(X_{TH} + X_{lr})}$$

$$I_r = \frac{V_{TH}}{\sqrt{(R_{TH} + R_r/s)^2 + (X_{TH} + X_{lr})^2}}$$

The developed electromagnetic torque can be determined through

$$
\begin{aligned}
T_e &= \frac{P_{mech}}{\omega_m} = \frac{P_{ag}(1-s)}{(1-s)\omega_s} = \frac{P_{ag}}{\omega_s} \\
&= \frac{3I_r^2 R_r}{s\omega_s}
\end{aligned}
$$

Which can be expressed in terms of the magnetizing electromotive force E and others:

$$T_e = \frac{3E^2(R_r/s)}{\omega_s[(R_r/s)^2 + X_{lr}^2]}$$

Or in terms of the Thevenin's circuit variables and others:

$$T_e = \frac{3V_{TH}^2 (R_r/s)}{\omega_s[(R_{TH} + R_r/s)^2 + (X_{TH} + X_{lr})^2]}$$

It is clear from the torque expression that given a fixed voltage-frequency supply (both V_s and ω_s are fixed), the torque's magnitude depends entirely on the slip s, i.e. indirectly on the motor speed, which is $(1\text{-}s)\omega_s$. As s changes from 1 to 0, the motor speed ω_m changes from 0 to ω_s. A typical plot of developed torque versus motor speed (T_e vs ω_m) is shown in Fig. 3.8, together other plots such as stator current versus motor speed (I_s vs ω_m), rotor current versus motor speed (I_r vs ω_m), mechanical output power versus motor speed (P_{mech} vs ω_m), and efficiency versus motor speed (η vs ω_m). P_{mech} expression can be derived accordingly as:

$$\begin{aligned} P_{mech} &= P_{ag}(1-s) \\ &= \frac{3V_{TH}^2 R_r (1-s)}{s[(R_{TH} + R_r/s)^2 + (X_{TH} + X_{lr})^2]} \end{aligned}$$

I_s expression can be derived accordingly as:

$$\boldsymbol{I_s} = \frac{\boldsymbol{V_s} - \boldsymbol{E}}{R_s + jX_{ls}}$$

Where the magnetizing back EMF can be computed from the supply voltage and the Thevenin's equivalent circuit:

$$\boldsymbol{E} = \left(\frac{R_r/s + jX_{lr}}{R_{TH} + R_r/s + j(X_{TH} + X_{lr})} \right) \boldsymbol{V_{TH}}$$

$$\boldsymbol{V_{TH}} = \frac{jX_m \boldsymbol{V_s}}{R_s + j(X_m + X_{ls})}$$

The relationship between the derived electrical variables and the motor slip are shown graphically in Fig. 3.8.

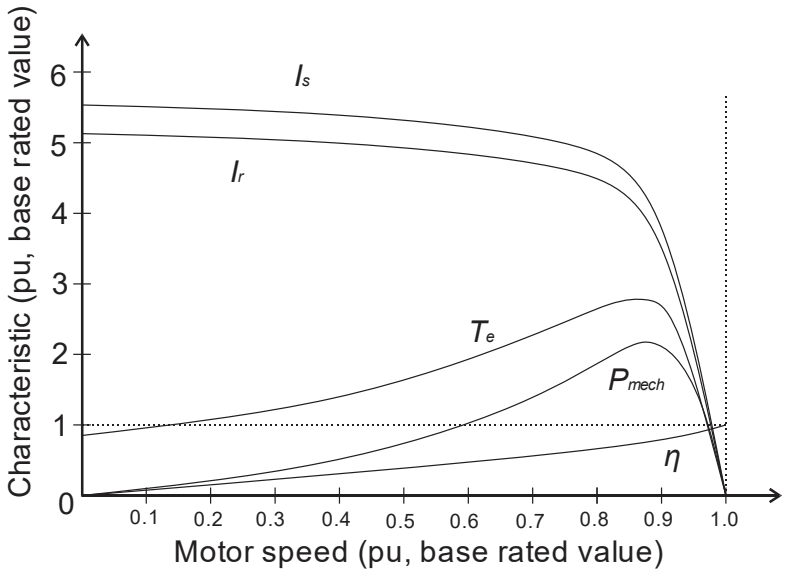

Fig. 3.8: Evolution of the currents, electromagnetic torque (T_e), stator current (I_s), rotor current (I_r), mechanical output power (P_{mech}), and efficiency (η) with the motor speed (ω_m).

Based on Fig. 3.8, we can also know that:

1) At small slip, the torque is nearly proportional to slip.
2) As slip increases (speed decreases), stator and rotor current increase.
3) There is a slip value that corresponds to a maximum torque value (a.k.a. pull-out torque or breakdown torque). This slip value is usually only a few percent less than the full slip 1.
4) When the load torque exceeds the breakdown torque, the motor will decelerate rapidly to zero. For protection of the circuitry, supply to the machine must be disconnected immediately.

The magnitude of the breakdown torque and the corresponding slip value are derived as follows. From torque expression derived earlier, the optimum value can be found by first-s-derivative equal to zero (some steps are skipped):

$$0 = \left.\frac{dT_e}{ds}\right|_{s=s_m}$$

$$0 = \frac{d}{ds}\left[\frac{3R_r V_{TH}^2 (R_r/s_m)}{\omega_s[(R_{TH}+R_r/s_m)^2+(X_{TH}+X_{lr})^2]}\right]$$

$$s_m = \pm\frac{R_r}{\sqrt{R_{TH}^2+(X_{TH}+X_{lr})^2}}$$

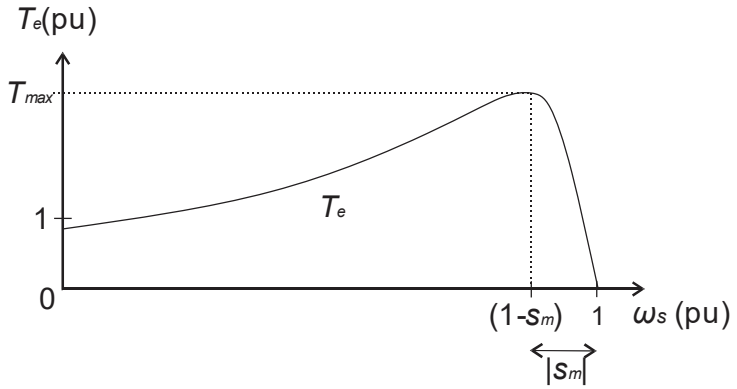

Fig. 3.9: Pull-out torque and the corresponding slip.

3.3. Speed control by simultaneous stator voltage and frequency variation

Apart from the natural torque/speed change resulted from loadings, the synchronous speed (and therefore also the motor's mechanical speed) and torque of the induction motor can be controlled by manipulating the stator voltage supply, in terms of its magnitude, frequency and/ or phase (note that the speed change through rotor circuit control will not be discussed here). A number of open-loop control methods have been developed over the past two decades and the most relevant method nowadays is the simultaneous stator voltage and frequency control, which is also known as variable-voltage-variable-frequency control or simply scalar control.

Consider that if the stator frequency is to be changed from ω_s to $\beta\omega_s$, where $0 < \beta \leq 1$, the maximum torque expression becomes:

$$T_{e@\beta\omega_s} = \frac{3V_{TH}^2(R_r/s)}{\beta\omega_s[(R_{TH}+R_r/s)^2+(\beta X_{TH}+\beta X_{lr})^2]}$$

Also, the magnitude of pull-out torque is obtained by substituting the positive slip into the torque expression to give:

$$T_{\max@\beta\omega_s} = \frac{3V_{TH}^2}{2\beta\omega_s[R_{TH}+\sqrt{R_{TH}^2+(\beta X_{TH}+\beta X_{lr})^2}]}$$

By assuming R_{TH} (i.e. R_s) is negligible compared to the reactance terms (which is usually a valid assumption for kW range motor), the maximum torque can be simplified to:

$$\begin{aligned} T_{\max@\beta\omega_s} &= \frac{3V_{TH}^2}{2\beta\omega_s(\beta X_{TH}+\beta X_{lr})} \\ &= \frac{3}{2\omega_s(X_{TH}+X_{lr})}\left(\frac{V_{TH}}{\beta}\right)^2 \end{aligned}$$

If V_{TH} is changed according to the same β ratio from V_{TH} to βV_{TH} as the frequency changes from ω_s to $\beta\omega_s$, the maximum torque can practically be maintained constant despite the change of frequency. For typical induction machines, $V_{TH} \approx V_s$, which would mean that if one were to change the voltage V_s and the frequency by the same ratio, the maximum torque attainable by the machine will remain almost constant. This is the fundamental principle for scalar control of induction motor which requires the speed (frequency) control be accompanied by an equivalent voltage magnitude changes. In ideal case, within the base speed region (i.e. below the rated frequency), the stator voltage should be reduced proportionally with the operating frequency; beyond the base speed region (usually known as field weakening region, with its maximum value typically capped at 2-4 times the rated frequency), the supply voltage will be kept constant and this also means that the magnetizing flux will be reduced and also the maximum torque attainable by the induction machine. These relationships are represented in Fig. 3.10.

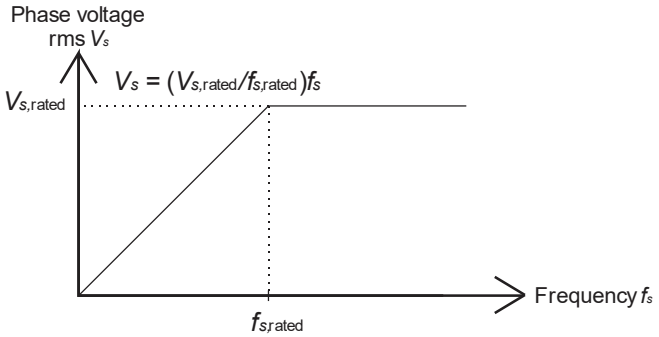

Fig. 3.10: Ideal *V/f* profile.

From Fig. 3.5, the following voltage balanced equation can be obtained:

$$E_m = V_s - (R_s + jX_{ls})I_s = jX_m I_m$$
$$V_s = jX_m I_m + (R_s + jX_{ls})I_s$$

Recall the relevance of the assumption $|X_m I_m| >> |R_s I_s + jX_{ls} I_s|$, the above equation can be simplified, and with some manipulation, the magnetizing current at rated supply frequency is approximated as:

$$V_s \approx X_m I_m$$
$$I_m \approx \frac{V_s}{X_m}$$

With a supply voltage of frequency $\beta\omega_s$ and magnitude βV_s, the magnetizing current can be approximated to be:

$$I_{m@\beta\omega_s} \approx \frac{\beta V_s}{\beta X_m} = \frac{V_s}{X_m} = I_{m@\omega_s}$$

This derivation hints that the magnetizing current I_m is kept almost constant by keeping the change in V_s and the change in ω_s to have the same ratio β. In other words, if the V_s/f_s ratio is kept constant, a constant air-gap flux as well as the pull-out torque (i.e. maximum achievable torque) can maintained about their rated values. This relation applies only to the base speed region. Beyond the synchronous speed, i.e. in the field weakening region, owing to limited supply voltage (which usually cannot be increased beyond the rated value for the integrity of the winding insulation), supply voltage V_s can be kept constant while the speed increases. This leads to lower V_s/f_s ratio and hence lower pull-out torque.

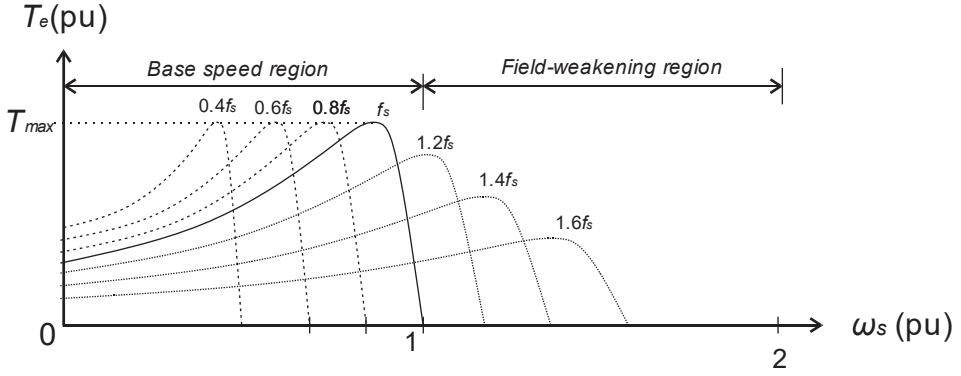

Fig. 3.11: Motor torque-speed curve at different operating frequencies but with constant V_s/f_s ratio before the synchronous frequency, and with reduced V_s/f_s ratio beyond the synchronous frequency.

The previous approximation is a valid at high speed near the synchronous speed. As speed decreases towards zero, the reactance components (X_m and X_{ls}) become smaller and the $R_s I_s$ component becomes increasingly significant compared to the decreasing V_s. In order to account for the resistive voltage drop, a voltage boost is usually introduced in practice, as illustrated by Fig. 3.12.

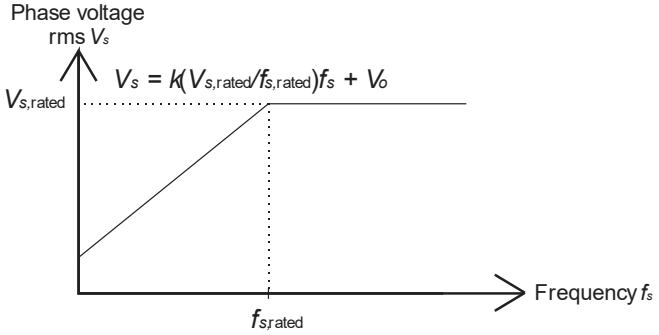

Fig. 3.12: Practical *V*/*f* profile with voltage boost, $k = (V_{s,rated} - V_o)/V_{s,rated}$.

This can be explained by examining the equivalent circuit. In order to keep the magnetizing current I_m to be constant, one actually would have to keep E_m constant (since $I_m = E_m/jX_m$) instead of V_s constant.

$$E_m = V_s - (R_s + jX_{ls})I_s = jX_m I_m$$

With that, the rotor excitation would remain practically the same, and the from the torque equation:

$$T_e = \frac{3I_r^2 R_r}{s\omega_s}$$

3.4. Inverter control of induction machines using sinusoidal PWM

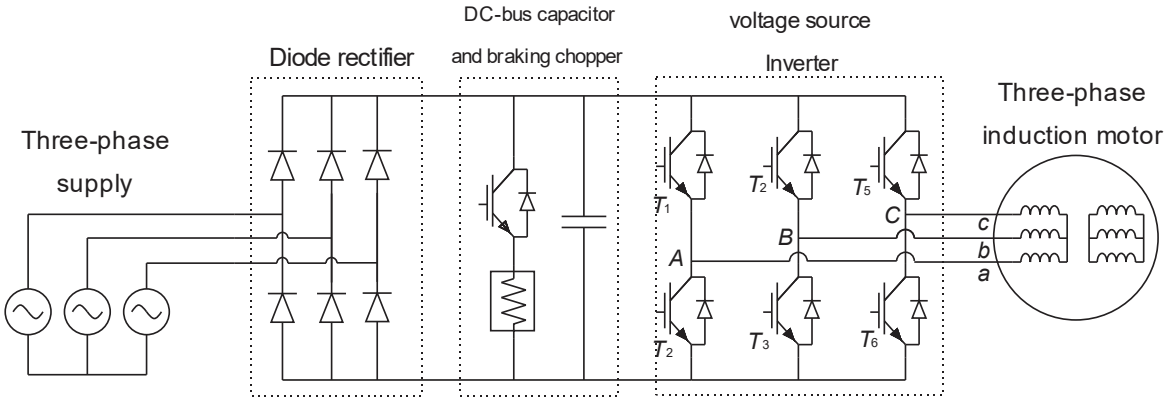

Fig. 3.13: A three-phase induction motor drive supplied by a diode-front-end two-level voltage source inverter.

The most common form of AC drives used in industry is of the voltage source type having typically three main components: rectifier, DC bus, and inverter. For low power drives, diode-based rectifier, a.k.a. diode front end, is the common topology. For medium-high power drives, active front end having the capability of feeding regenerated power back to the grid is used. The DC-bus capacitor smoothens the rectified AC to give a practically constant DC-bus voltage. For diode front end, if the induction motor-load system is of large inertia, a braking chopper is normally needed to maintain the DC-bus voltage to within the permissible level by disposing the regenerated energy to the power resistor. The fundamental principle is somewhat similar to the DC drive's regenerative feedback.

Variation of both inverter output voltage and output frequency as explained by the preceding section is now achieved by the voltage source inverter operated with sinusoidal pulse width modulation (PWM). There are three inverter legs as shown in Fig. 3.13. Modulation signal for each leg is obtained by comparing a sinusoidal reference signal to a triangular carrier: if the reference signal greater than the carrier signal, the output signal is 1; otherwise, the output signal is 0. The carrier has a frequency of f_c, which is normally at least tens of times greater than the nominal frequency of the reference signal's frequency f_s. The voltage reference signal is obtained by normalizing the desired phase voltages with the peak voltage, $V_{b,pk}$, calculated from:

$$V_{b,pk} = \frac{V_{dc}}{2}$$

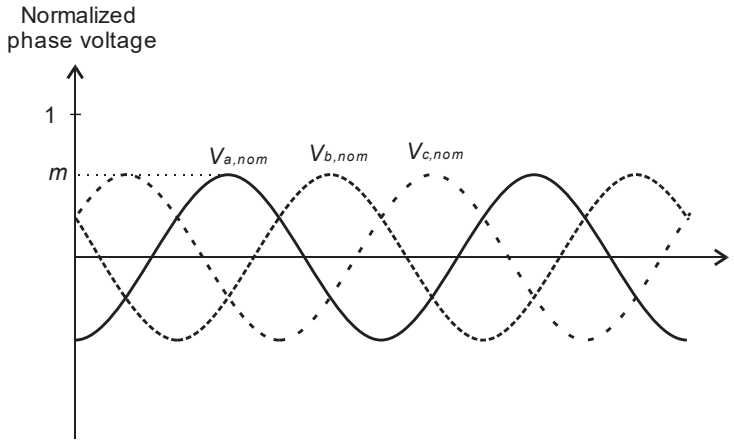

Fig. 3.14: Normalized three-phase voltage waveforms.

Fig. 3.14 shows an example of three-phase voltage reference signals of amplitude m. These voltages are obtained by normalizing the original voltage waveforms with amplitude $mV_{b,pk}$. m is normally referred to as the modulation index of the reference signal, taking the value between $0 < m \leq 1$. Fig. 3.15 shows the generation of leg-A switching signals from the phase-a voltage reference signal and the universal carrier signal (used by all three phases/legs, and of an intentionally reduced frequency for visualization purpose). Fig. 3.16 shows the reference signal examples at two different frequencies (one higher, one lower) than the previously discussed signal.

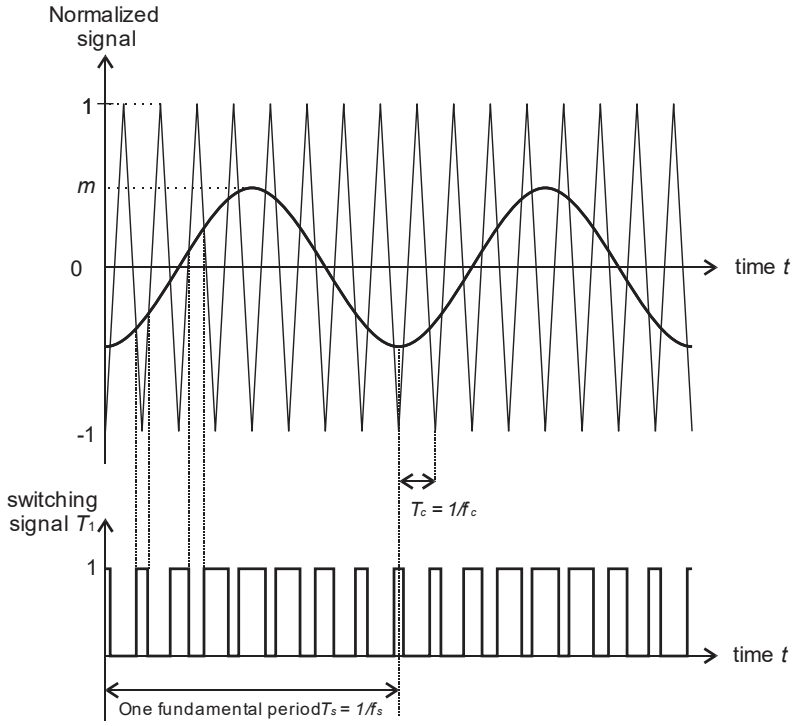

Fig. 3.15: Normalized phase-a voltage of amplitude ($mV_{b,pk}$) is compared against the triangular carrier of frequency f_{sw} to generate the leg-A's T_1 switching signal. Leg-A's T_2 switching signal is complementary to that of T_1.

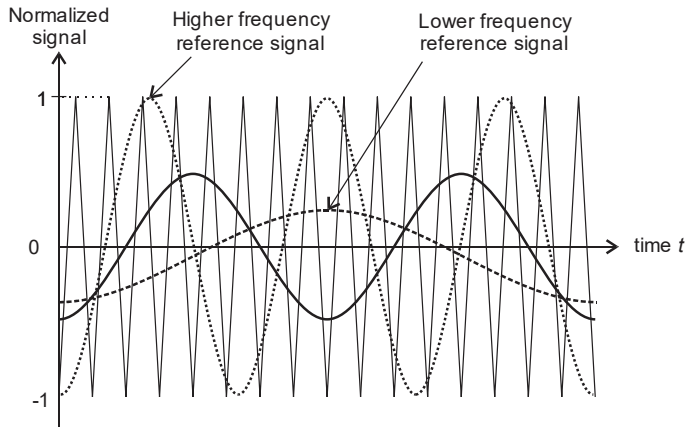

Fig. 3.16: An example showing reference signal with different frequency (and hence amplitude, following the *V*/*f* control law)

Fig. 3.17 below shows a case study consisting a scalar control drives supplying a star-connected 2.2kW three-phase induction motor with open-neutral (means the neutral point is left unconnected). The AC drives is supplied by the standard 415V 50Hz AC mains. Assume that the DC-bus capacitance is large enough, the DC-bus voltage at no-load is V_{dc} = 415√2=587V. Hence the leg-voltage waveform consists of a train of pulses of amplitude 0 and V_{dc}. On the other hand, the phase-voltage is obtained by measuring across each phase with respect to the neutral point. These voltage waveforms consist of trains of pulses with amplitude (2/3)V_{dc}, (1/3)V_{dc}, 0, -(1/3)V_{dc}, and -(2/3)V_{dc}. These voltages are commonly known as quasi-sinusoidal voltages. Determining the exact fourier expression to represent the inverter output voltage is beyond the scope (as it very much depends on the type of modulation technique, type of edge, type of sampling, etc, and each would have a very different expression). One example is shown below to illustrate the complex expression for the phase-to-neutral expression for a standard sinusoidal PWM technique:

$$V_o(\omega_s t) = V_{dc} + mV_{dc}\cos(\omega_s t - \frac{k\cdot 2\pi}{3}) + \frac{4V_{dc}}{\pi}\sum_{n=+1}^{+\infty}\sum_{p=-\infty}^{+\infty}\left[\sin(n+p)\frac{\pi}{2}\right]\frac{J_p\left(\frac{n\pi}{2}m\right)}{n}\cos\left[n(\omega_c t+\varphi_c)+p(\omega_s t-\frac{k\cdot 2\pi}{3})\right]$$

Despite their significant voltage harmonic content, only the low-order harmonic is capable of exciting the corresponding currents in the machines, while the high-order voltage harmonics (of f_c range, usually in kHz range) cannot excite large currents due to high impedance (reactance becomes very large at kHz range).

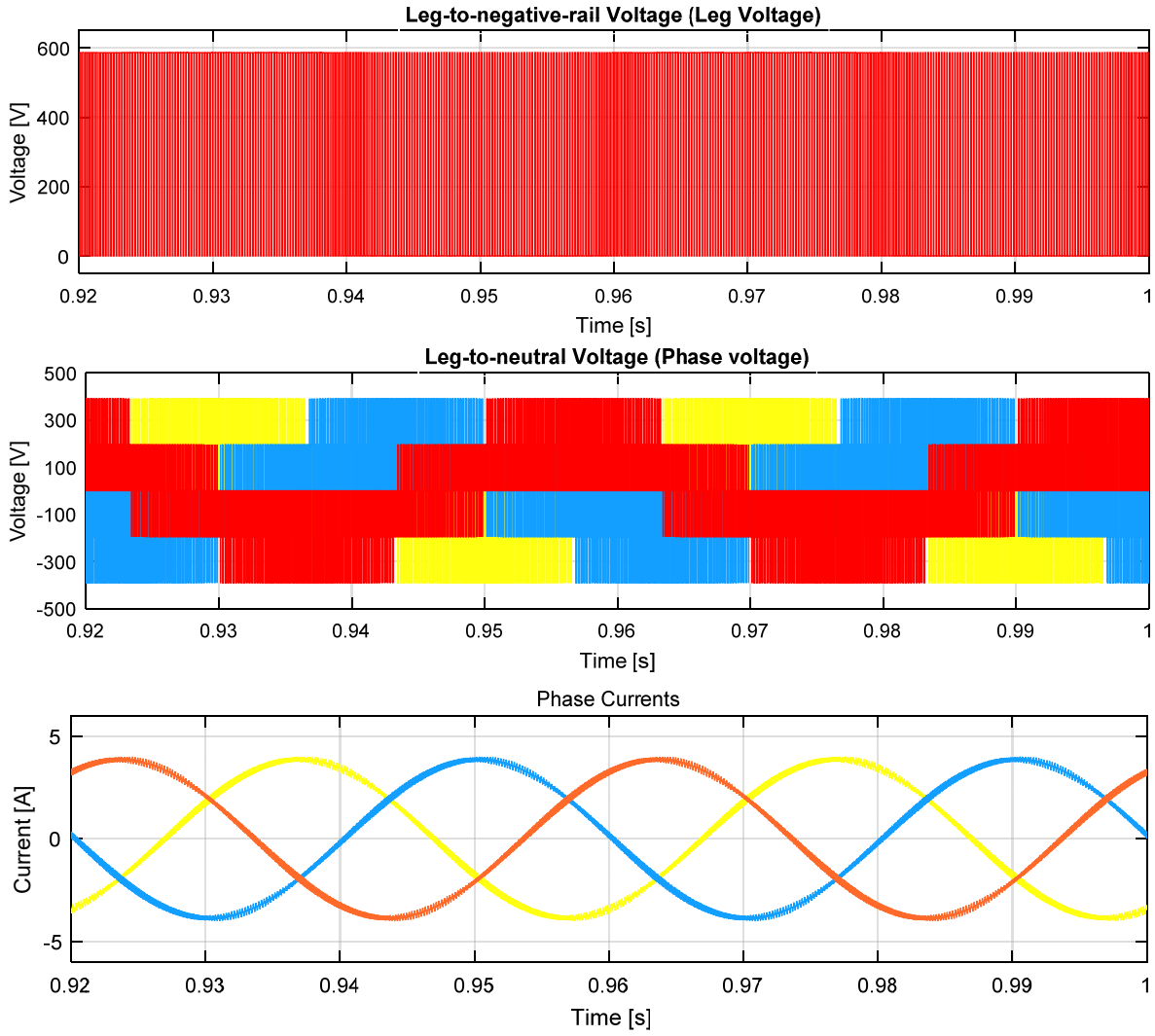

Fig. 3.17: Voltage and current at 25Hz operation with a 5Nm load. (Top) Inverter leg-*A* voltage waveform; (middle) phase voltages, measured with respect to the motor neutral point; (bottom) phase currents.

3.5. Dynamic control of induction machines using voltage source inverters (an introduction)

Induction motor is a singly fed machine, which means it only requires a single supply to operate, unlike the separately excited DC machine or synchronous machines. The speed control principle introduced in Section 3.3 can realize a variable speed motor which would meet the slow speed-changing requirement of applications such as conveyor belt, fans, and pumps. In conventional fans and pumps, if variable air/fluid flow speed is required, mechanical valves are introduced to control it on the on-off basis or on the modulation basis. If variable speed drive is used, then this conventional valve-based flow control can be removed, which then leads to energy saving.

On the other hand, in some applications the high dynamic speed/torque control of the motor could be one of the design requirement for the application. Examples include lift, paper mill's double-drum winder, electric vehicle, ship propulsion, and also power control in wind power generation's machine (doubly fed induction machine operating in the generating mode). Fundamentally, in order to achieve high dynamic speed control, one will have to control the

electromagnetic torque of the induction motor which is physically non-linear. The early advancement of high-performance motor drives research have laid out a series of model ling and control principle which would enable the non-linear torque of a three-phase induction motor to be controlled dynamically. There are several established methods and the most common and commercially available are: field oriented control and direct torque control. The principle of the field oriented control is based on an analogy to the separately excited DC motor in which is flux is controlled by the field current and the torque is controlled independently by the armature current (given a constant flux current). So it can be said that the flux and torque producing currents are electrically and magnetically separated. On the contrary, an induction motor has a single three-phase supply (at the stator), so naturally the flux and torque of the machine are coupled together. This coupling can be removed by decomposing the instantaneous current into two components: flux-producing current and torque-producing current, in an arbitrarily chosen reference frame synchronized to the magnetic flux. In fact this simple concept also forms the basis for numerous converter-based power control in renewable energy technology such as wind and solar power control (outside the scope of this chapter). Mathematical treatment of high performance control method is presently outside the scope of this module. Fig. 3.18 below gives a good overview of variable speed/frequency control for induction motors. Interested readers are referred to advanced reference books such as *Power Electronics - Circuits, Devices, and Applications* (3rd ed., Pearson, 2003) by M. H. Rashid and *Sensorless Vector and Direct Torque Control* (Oxford University Press) by Peter Vas.

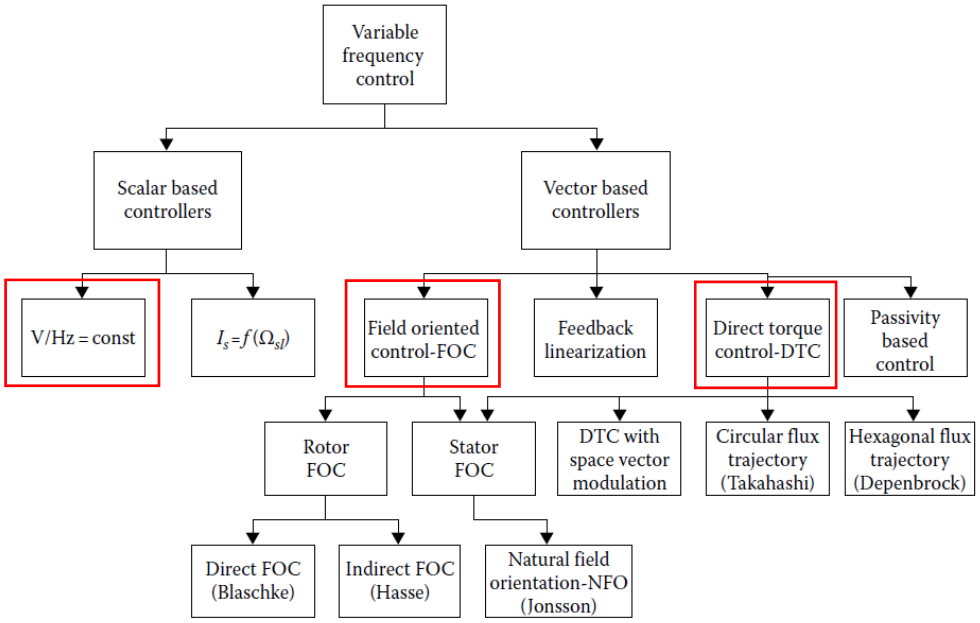

Fig. 3.18: General classification of induction motor control methods. The red-square-circled methods are the commercial induction motor methods being used widely in the industry.

3.6. Tutorial

(1) A three-phase 460V 60Hz star-connected induction motor is supplied from a three-phase voltage source inverter that is operated by sinusoidal PWM. Calculate the input DC voltage required. [678V]

(2) A three-phase 400V 50Hz 6-pole 960 rpm start-connected induction motor has the following parameters: R_s = 0.4Ω, R_r = 0.2Ω, X_{ls} = 1.5Ω, X_{lr} = 1.5Ω, and X_m = 30Ω. The motor is connected to a rated supply.